How grooves reflect and confine surface plasmon polaritons

Martin Kuttge,[1,*] F. Javier García de Abajo,[2] and Albert Polman[1]

[1]*Center for Nanophotonics, FOM-Institute AMOLF, Sciencepark 113, 1098 XG Amsterdam, The Netherlands*
[2]*Instituto de Óptica - CSIC, Serrano 121, 28006 Madrid, Spain*
**kuttge@amolf.nl*

Abstract: The reflection of surface plasmon polaritons by deep linear grooves structured into gold surfaces is investigated with numerical finite-difference-in-time-domain as well as boundary-element-method calculations. Groove widths of 25 and 100 nm are studied, with depths as large as 500 nm. The reflection depends strongly on wavelength, groove depth, and width. By systematically varying these parameters and studying the field profiles in the grooves as well as mode dispersion, we relate the resonances of the reflectivity to resonant coupling of propagating planar plasmon modes to cavity modes inside the grooves. By careful design of the groove width and depth the reflectivity can be tuned to values up to at least 30% for either a narrow or wide band of wavelengths.

OCIS codes: (240.0668) Surface Plasmons; (250.5403) Plasmonics.

References and links

1. H. Raether, *Surface Plasmons on Smooth and Rough Surfaces and on Gratings*, (Springer, 1988).
2. S. I. Bozhevolnyi, V. S. Volkov, E. Devaux, J.-Y. Laluet, and T. W. Ebbesen, "Channel plasmon subwavelength waveguide components including interferometers and ring resonators," Nature **440**(7083), 508–511 (2006).
3. J.-C. Weeber, Y. Lacroute, A. Dereux, T. W. Ebbesen, C. Girard, and M. U. Gonzalez, and A.-L. Baudrion, "Near-field characterization of Bragg mirrors engraved in surface plasmon waveguides," Phys. Rev. B **70**(23), 235406 (2004).
4. M. U. Gonzalez, J.-C. Weeber, A.-L. Baudrion, A. Dereux, A. L. Stepanov, J. R. Krenn, E. Devaux, and T. W. Ebbesen, "Design, near-field characterization, and modeling of 45° surface-plasmon Bragg mirrors," Phys. Rev. B **73**(15), 155416 (2006).
5. J. A. Sánchez-Gil, and A. A. Maradudin, "Surface-plasmon polariton scattering from a finite array of nano-grooves/ridges: Efficient mirrors," Appl. Phys. Lett. **86**(25), 251106 (2005).
6. M. Kretschmann, and A. A. Maradudin, and A. A. Maradudin, "Band structures of two-dimensional surface-plasmon polaritonic crystals," Phys. Rev. B **66**(24), 245408 (2002).
7. F. Pincemin, and J.-J. Greffet, and J.-J. Greffet, "Propagation and localization of a surface plasmon polariton on a finite grating," J. Opt. Soc. Am. B **13**(7), 1499–1509 (1996).
8. J. A. Sánchez-Gil, "Surface defect scattering of surface plasmon polaritons: Mirrors and light emitters," Appl. Phys. Lett. **73**(24), 3509–3511 (1998).
9. A. Y. Nikitin, F. Lopez-Tejeira, and L. Martin-Moreno, "Scattering of surface plasmon polaritons by one-dimensional inhomogeneities," Phys. Rev. B **75**(3), 035129 (2007).
10. W.-C. Tan, T. W. Preist, J. R. Sambles, and N. P. Wanstall, "Flat surface-plasmon-polariton bands and resonant optical absorption on short-pitch metal gratings," Phys. Rev. B **59**(19), 12661–12666 (1999).
11. E. K. Popov, N. Bonod, and S. Enoch, "Comparison of plasmon surface waves on shallow and deep metallic 1d and 2d gratings," Opt. Express **15**(7), 4224–4237 (2007).
12. J. Le Perchec, P. Quémerais, A. Barbara, and T. López-Ríos, "Why metallic surfaces with grooves a few nanometers deep and wide may strongly absorb visible light," Phys. Rev. Lett. **100**(6), 066408 (2008).
13. P. Lallane, J. P. Hugonin, and J. C. Rodier, "Approximate model for surface-plasmon generation at slit apertures," J. Opt. Soc. Am. A **23**(7), 1608–1615 (2006).
14. E. D. Palik, *Handbook of Optical Constants*, (Academic Press, 1985).
15. F. J. García de Abajo, and A. Howie, "Relativistic electron energy loss and electron-induced photon emission in inhomogeneous dielectrics," Phys. Rev. B **65**, 115418 (2002).
16. K. Vahala, *Optical Microcavities*, (World Scientific, 2004).
17. E. Moreno, F. J. Garcia-Vidal, S. G. Rodrigo, L. Martin-Moreno, and S. I. Bozhevolnyi, "Channel plasmon-polaritons: modal shape, dispersion, and losses," Opt. Lett. **31**(23), 3447–3449 (2006).
18. I. V. Novikov, and A. A. Maradudin, "Channel polaritons," Phys. Rev. B **66**(3), 035403 (2002).

#109987 - $15.00 USD Received 13 Apr 2009; revised 18 May 2009; accepted 26 May 2009; published 5 Jun 2009

19. J. Dionne, L. Sweatlock, H. A. Atwater, and A. Polman, "Planar metal plasmon waveguides: frequency-dependent dispersion, propagation, localization, and loss beyond the free electron model," Phys. Rev. B **72**(7), 075405 (2005).

1. Introduction

Recent advances in nanoscale structuring have opened up new possibilities in the field of nanophotonics. Surface plasmon polaritons (SPPs) [1] can be employed as a way to improve the performance and reduce the size of photonic circuits. The two-dimensional character of SPPs makes it possible to confine electromagnetic radiation below the diffraction limit, offering unprecedented possibilities for subwavelength photonics [2].

Reflectors for SPPs are important elements in plasmonic integrated circuits, as they allow guiding and steering of SPPs and constitute basic building blocks for plasmonic resonators. Grating-like Bragg reflectors consisting of arrays of parallel shallow grooves or ridges are widely used as reflecting components and a large effort has been devoted to their optimization [3]. Reflectivity values of almost up to 100% have been reported experimentally for reflectors spanning tens of grating periods [4]. Single grooves structured into the surface can also act as a reflector for SPPs and have much smaller size.

While the theoretical work on the reflectivity of Bragg reflectors is extensive [5–7], the reflectivity of single grooves has not been investigated in much detail. Moreover, only a limited range of groove geometries have been studied. Existing studies are mainly restricted to shallow grooves that are susceptible to be examined within a perturbation approach. Sánchez-Gil [8] showed results on reflectivity and emissivity of shallow grooves while Nikitin *et al.* [9] reported on the reflectivity and scattering coefficients of shallow grooves for normal in-plane incidence. Further work on grooves in metal surfaces focused mainly on the absorption properties of light by grooved surfaces [10–12] or SPP generation by light beams incident onto a single groove [13] rather than SPP reflection.

In this paper we investigate the possibility of using single grooves as efficient reflectors for surface plasmons. We show that suitably designed deep single grooves can perform as efficient and broadband reflectors for SPPs. We have used finite-difference-in-time-domain as well as boundary-element-method calculations to determine the reflectivity for grooves with varying geometrical parameters. We show that the observed high reflectivity is a result of efficient coupling of propagating planar modes to resonant groove modes.

2. Reflectivity of single grooves

We used two-dimensional finite-difference-time-domain (FDTD) calculations to obtain the reflection coefficient of surface plasmons incident onto a groove structured into an otherwise planar gold surface. The system was modeled as an infinite box with the optical constants of gold taken from Palik [14]. A groove was structured with a profile similar to the ones used in experimental studies. In particular, the groove profile is composed of two quarter-circles with radius r = 50 nm and a half-ellipse with minor radius $a = w/2$ equal to half the groove width and the major radius equal to $b = d-r$, with d the groove depth (see inset of Fig. 1(a)). A surface plasmon was launched at a distance of 1 μm from the groove edge under normal incidence. The transmission through the groove was monitored with a frequency domain monitor positioned at the far side of the groove while the reflection was recorded with a monitor behind the source. The grid size for the calculations was 3 nm and was refined around the surface layer and the groove to 0.9 nm. The simulation region was bound by perfectly matched layers (PMLs) to absorb SPPs leaving the region of interest. The reflectivity of the PML was found to be smaller than 0.1% and therefore did not significantly influence our results.

In Fig. 1 we show the reflectivity of the groove as a function of groove depth and wavelength for groove widths (a) w = 25 nm and (b) w = 100 nm, respectively. For both widths we observe maxima of the reflectivity that depend on wavelength and groove depth. The highest reflectivity (29%) is observed for the 100 nm wide grooves and appears for groove depths of 100-120 nm at wavelengths between 600 and 750 nm. For the 25 nm wide

#109987 - $15.00 USD Received 13 Apr 2009; revised 18 May 2009; accepted 26 May 2009; published 5 Jun 2009

groove a nearly as high reflectivity maximum (25%) is found in the same wavelength range, for slightly smaller groove depth. The reflectivity maxima in Fig. 1 roughly show a linear trend with increasing groove depth. The narrower groves (a) are much more dispersive than the wider ones (b) as more maxima are observed for the same wavelength. Moreover, maxima for deeper grooves show a slightly narrower width of the reflectivity resonances.

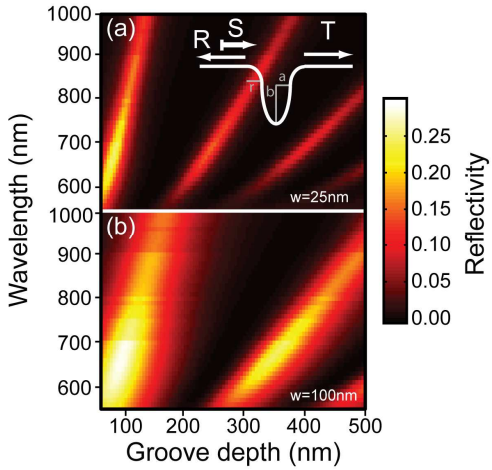

Fig. 1. Reflectivity for surface plasmons incident perpendicularly onto a groove structured into a gold surface as a function of groove depth and wavelength calculated using FDTD. Groove width: (a) 25 nm; (b) 100 nm. The inset shows a schematic of the groove shape.

3. Reflectivity and field enhancement

To gain insight into the origin of the reflectivity maxima, we have computed the local field inside a 25 nm wide, 500 nm deep groove at the wavelength of maximum reflectivity (640 nm). We used the boundary element method (BEM) to calculate the local magnetic field [15]. The magnetic near-field intensity calculated for a plasmon incident from the left onto the groove is shown in the main panel of Fig. 2. Inside the groove, a standing wave pattern can be observed and the maximum field intensity is a factor of three higher than for the incoming plasmon. The inset in Fig. 2 shows the magnetic field intensity for a 70 nm deep groove (first reflection maximum). At this depth, the field is mainly concentrated at the bottom of the groove. The arrows in Fig. 2 represent the Poynting vector, which shows the energy flux in the system. Away from the groove, the energy flows from left to right, the direction of SPP propagation. Near the groove, the Poynting vector is directed towards the groove, so that energy is transmitted into the groove. This is a clear signature of coupling between planar surface plasmons and a localized mode confined in the groove.

To further investigate the relation between enhanced reflectivity and coupling of SPPs to groove modes, we have compared the field inside the groove to the reflectivity. Figure 3(a) shows the reflectivity as a function of groove depth at a free-space wavelength of 640 nm (a horizontal cross-cut in Fig. 1). Also plotted is the electric field intensity integrated over the area of the groove and then normalized to that area. Clearly, maximum reflectivity and maximum field intensity are observed at the same groove depth. In Fig. 3(b) we show reflectivity and average field intensity as a function of wavelength for fixed groove depth (500 nm) and width (25 nm). Here too, the calculated wavelengths of the maximum in both curves agree very well. From the data in Fig. 3 we can conclude that the increased reflectivity is related to efficient coupling of the incident planar SPPs to resonant groove modes.

#109987 - $15.00 USD Received 13 Apr 2009; revised 18 May 2009; accepted 26 May 2009; published 5 Jun 2009

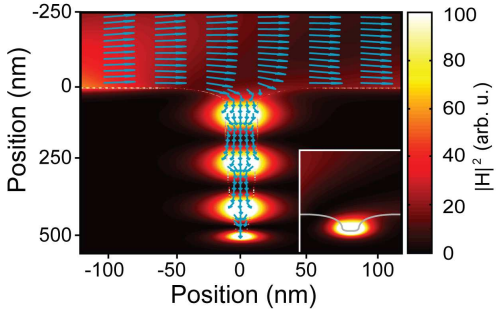

Fig. 2. Magnetic field intensity calculated with the boundary element method for a 500 nm deep groove at a wavelength of 640 nm. The SPP was launched by an incoming electron impacting 2900 nm to the left of the groove. The blue arrows denote the Poynting vector. Inset: Magnetic field intensity for a 70 nm deep groove at the same wavelength.

On resonance, surface plasmons are coupled into the groove to excite a localized groove mode. The re-radiation of the energy stored in the groove cavity into forward and backward emission is observed as transmission and reflection, respectively. In this model, the coupling of the incident plasmon wave with the resonant groove mode is similar to Rayleigh scattering of a plane wave with a point dipole that leads to forward and backward radiation.

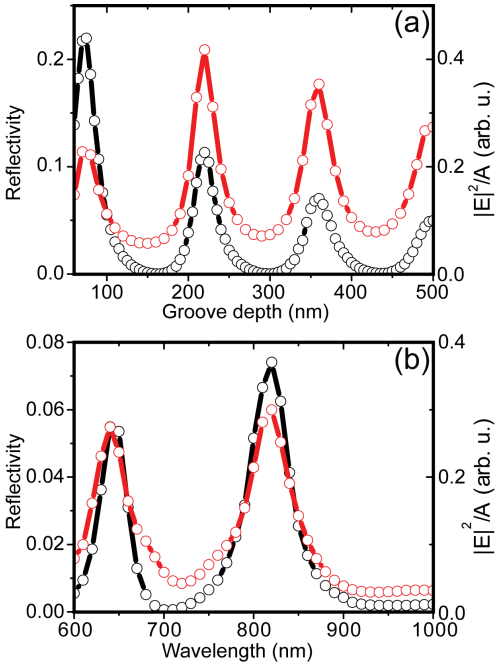

Fig. 3. Black curves and symbols: FDTD calculations of the reflectivity for surface plasmons incident perpendicularly onto a groove structured into a gold surface as a function of groove depth. Red curves and symbols: Electric field intensity integrated over the area *A* of the groove as calculated from BEM. (a) Calculations as a function of groove depth at a free-space wavelength of 640 nm for a 25 nm wide groove; (b) Calculations as a function of wavelength for a 500 nm deep, 25 nm wide groove.

The phase difference between the SPPs transmitted trough the groove and the directly transmitted SPPs is determined by the groove geometry. If the groove geometry could be designed such that those two parts are equal in magnitude but are out of phase, the

#109987 - $15.00 USD Received 13 Apr 2009; revised 18 May 2009; accepted 26 May 2009; published 5 Jun 2009

transmission will vanish and full reflection will be observed. This condition is similar to critical coupling observed for optical microcavities [16]

4. Coupling to groove modes

The coupling between the propagating plasmon and the localized groove mode becomes clearer when we investigate the depth-profile of the observed groove-mode field. In Fig. 4 we plot the electric field intensity profile along a line in the center of the groove (a vertical cross-cut through Fig. 2) for different wavelengths and as a function of position. The groove depth is 500 nm, the groove width 25 nm, and the field is normalized to its maximum value for each wavelength. The wavelengths of maximum groove reflectivity (see Fig. 3) are marked as dashed lines in the graph. For each wavelength, a standing wave pattern is observed with the position of high field intensity moving upwards for increasing wavelength. For the marked wavelengths of maximum reflectivity, a maximum of the electric field intensity reaches the upper end of the grooves. The increased field at the groove opening enables efficient coupling of incident SPPs to the standing groove mode. The higher intensity at the bottom of the grooves for all wavelengths is due to the stronger confinement of the plasmons as the grooves become narrower (see Fig. 1).

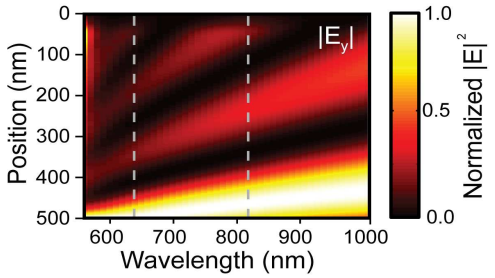

Fig. 4. Calculated electric field along a line in the center of a groove as a function of wavelength and position for a 500nm deep, 25nm wide groove in gold. For each wavelength the field was normalized to its maximum. The dashed lines indicate the wavelengths of maximum reflectivity from Fig. 3(b).

Propagating plasmon modes inside narrow grooves are known as channel plasmon polaritons (CPPs) [2,17,18]. The standing groove modes observed here are the special case of CPPs for $k_z = 0$, where k_z is the wavevector along the propagation direction along the length of the groove (i.e. normal to the plane of the cross section in Fig. 2). Using BEM calculations we determined the photonic local density of states (LDOS) as a function of wave vector and frequency inside the groove. A groove mode appears as a maximum in the LDOS. We have determined the wavelength of maximum LDOS for each wavevector to obtain the groove mode dispersion relation. In Fig. 5(a) we show the dispersion relation for 300 nm and 500 nm deep grooves with a width of 25 nm. Also plotted are the planar SPP dispersion and the light line in air. We observe flat dispersion bands starting at $k = 0$ and crossing the light line. While the low energy branches of the dispersion relation for the two depths overlap, higher-order-mode branches are well separated.

#109987 - $15.00 USD Received 13 Apr 2009; revised 18 May 2009; accepted 26 May 2009; published 5 Jun 2009

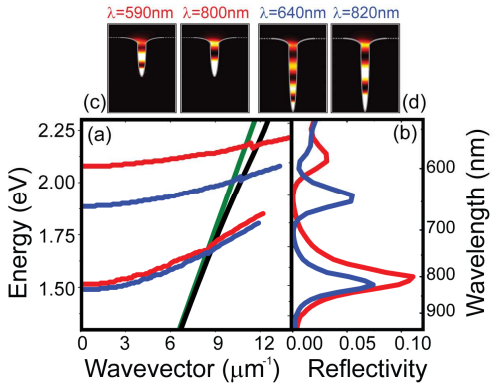

Fig. 5. (a) Dispersion relation for plasmons propagating in 300 nm (red line) and 500 nm (blue line) deep grooves with a width of 25 nm calculated using BEM. Light line in air (green) and single Au/air interface SPP dispersion (black). (b) FDTD calculations of the reflectivity as a function of wavelength for SPPs incident perpendicular onto a 300 nm (red line) and 500 nm (blue line) groove. (c) Electric field intensity inside a 300 nm deep groove at wavelengths of maximum reflectivity (590 and 800 nm). (d) Electric field intensity inside a 500 nm deep groove at wavelengths of maximum reflectivity (640 and 820 nm).

In Fig. 5(b) we plot the reflectivity for the same groove depths as a function of wavelength. The crossings of the dispersion relation branches with the origin $k_z = 0$ agree very well with the observed maxima in reflectivity, indicating that for normal incidence the incoming plasmon is indeed coupled to a standing $k_z = 0$ wave inside the groove. Note that for non-normal incidence the plasmon can couple to a channel plasmon propagating along the groove. This case is not studied here.

The electric field intensity profile associated to each wavelength of maximum reflection is shown in Fig. 5(c) and (d). We observe the standing wave pattern for each mode with increasing mode order for decreasing wavelength.

5. Grooves as MIM cavities

The spectral width of the reflectivity maxima in Fig. 1 depends on the groove width. Broad- or narrow-band reflection can thus be obtained by tuning the groove width. To investigate the relation between groove width and resonance line width, we have modeled the grooves as cavities of metal-insulator-metal (MIM) plasmons. The width of the observed resonances is determined by the cavity quality factor Q which describes the cavity losses. The cavity losses can be separated into losses which occur due to non-unity reflectivity at the cavity ends and due to the propagation loss of a plasmon inside the cavity due to Ohmic losses.

We have used the analytical solution for the MIM dispersion relation to determine the propagation losses [19]. The propagation loss was calculated from the imaginary part k_i of the wave vector. As expected, for the same frequency we observe a larger real part of the wave vector and high losses for the 25 nm wide waveguide compared to the 100 nm wide waveguide. In order to determine the reflectivity of the open and closed end of the groove we have performed FDTD calculations. For each groove width, an MIM plasmon mode was injected into a MIM waveguide, with the spacing between the metal interfaces equal to the groove width. The MIM waveguide was terminated either with an open or closed end having the same shape as the groove ends, and the reflection from the end was monitored. While at the closed end a high value of reflectivity is found for the 100 nm waveguide (~91%) compared to the 25 nm waveguide (~72%), at the open end the reflectivity is high for the 25 nm waveguide (~51%) compared to (~21%) for 100 nm.

#109987 - $15.00 USD Received 13 Apr 2009; revised 18 May 2009; accepted 26 May 2009; published 5 Jun 2009

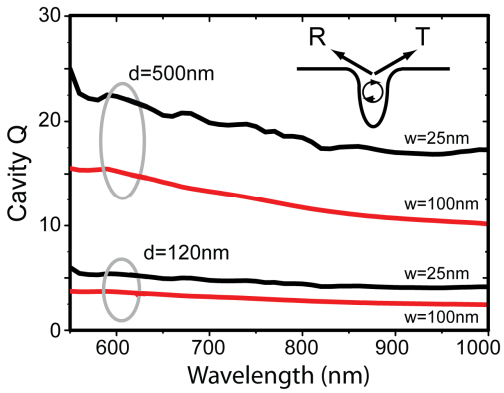

Fig. 6. Cavity quality factor Q for 25 nm (black) and 100 nm (red) wide grooves with depths of 120 nm and 500 nm. Q was calculated from FDTD calculations of the groove end reflection coefficients and propagation losses for MIM plasmons.

The quality factor of the cavity Q is defined by the ratio between the energy stored in the cavity and the energy loss per optical cycle. Equivalently, the quality factor can be determined by the round trip time, the optical frequency, and the fractional energy loss per cavity round trip. The energy loss ΔI per cavity round trip for a groove with depth d can be estimated as $\Delta I = I_0(1-R_oR_cexp(-4k_id))$, where R_o and R_c are the reflectivity at the open and closed ends, respectively. With the calculated propagation and reflection losses we have determined the theoretical Q for cavities with depths of 100 nm and 500 nm and widths of 25 nm and 100 nm; the results are shown in Fig. 6 as a function wavelength. The highest cavity quality factor Q = 25 is observed for 25 nm wide and 500 nm deep grooves. The fact that for the same width a higher Q is observed for deeper grooves indicates that the cavity losses are dominated by the reflectivity losses. The values of the cavity Q for 25 nm wide and 500 nm deep grooves agree reasonably well with the line width observed in Fig. 3(b). The higher calculated Q for the narrower cavity is in good agreement with the observed smaller resonance width in the reflectivity plots of Fig. 1 and is thus related to the higher cavity mode reflectivity for narrower cavities.

Using the model of an MIM cavity, we can assign mode numbers to the observed reflection maxima as described by *Tan et al.* [9]. The n^{th} mode of these grooves is given by the condition that the phase change that the plasmon picks up in a roundtrip within the groove is $\phi_n = (n-0.5)\pi$. From this condition we can estimate the position of the reflectivity maxima for a wavelength of 640 nm as shown in Fig. 3(a) to be at depths of 85 nm ($n = 1$), 227 nm ($n = 2$), 368 nm ($n = 3$), and 508 nm ($n = 4$), in good agreement with our FDTD results. This way we can explain the linear spectral dependence of the reflection maxima which follow the dispersion relation of MIM plasmons. Indeed, for shorter wavelength the stronger bending of the MIM dispersion relation can also be observed for the reflection maxima. This model agrees well with our observation in Fig. 4 that a reflection maximum occurs whenever a maximum of the field intensity reaches the upper groove edge or equivalently a multiple of the plasmon wavelength fits into the groove.

6. Summary

In conclusion, we have shown that single linear grooves in a planar gold surface can exhibit high reflectivity for incoming surface plasmon polaritons. The observed reflectivity shows resonances depending strongly on wavelength, groove depth and width, and a maximum reflectivity of 29% is observed. The reflectivity displays resonances that can be attributed to coupling with localized SPP modes inside the groove cavity. The highest cavity quality factor Q for the studied geometries is Q = 25. By engineering the coupling phase between an incoming SPP and the groove resonance, higher reflectivity may be obtained. These results are important to design suitable grooves acting as efficient reflectors for surface plasmons.

#109987 - $15.00 USD Received 13 Apr 2009; revised 18 May 2009; accepted 26 May 2009; published 5 Jun 2009

Acknowledgements

This work is part of the research program of "Stichting voor Fundamenteel Onderzoek der Materie" (FOM), which is financially supported by the "Nederlandse Organisatie voor Wetenschappelijk Onderzoek" (NOW)." F.J.G.A. acknowledges support from the Spanish MEC (Contract No. MAT2007-66050).

#109987 - $15.00 USD Received 13 Apr 2009; revised 18 May 2009; accepted 26 May 2009; published 5 Jun 2009